JOURNAL OF APPLIED ELECTROCHEMISTRY **28** (1998) 433–439

Corrosion protection of aluminium in acidic chloride solutions with nontoxic inhibitors

M. METIKOŠ-HUKOVIĆ, R. BABIĆ,

Department of Electrochemistry, Faculty of Chemical Engineering and Technology, University of Zagreb, Savska 16, POB 177, 10000 Zagreb, Croatia

Z. GRUBAČ

Department of Inorganic Chemistry, Faculty of Technology, University of Split, N.Tesle 10, 21000 Split, Croatia

Received 9 December 1996; revised 26 March 1997

Corrosion kinetics of 99.6% aluminium covered by a thin spontaneously formed oxide film in hydrochloric acid solution with and without the presence of substituted *N*-aryl pyrroles was studied using electrochemical impedance spectroscopy and quasi steady-state polarization. Measurements were performed on a rotating disc electrode in an argon-deaerated solution in the temperature range 20 to 50 °C. The addition of inhibitor considerably increases overvoltage of the cathodic process (HER) and shifts E_{corr} to negative potential values. The activation energy of the hydrogen evolution reaction was $E_a = 50 \pm 5$ kJ mol^{-1} and was not affected by the presence of inhibitor. The inhibitory action occurs by π-bonding between the adsorbed inhibitor molecules and the electrode surface. The electrode coverage follows the Langmuir adsorption isotherm with an adsorption equilibrium constant $K = 1.1$–2.64×10^5 dm^3 mol^{-1}. The adsorption of organic compound prevents the adsorption of chloride ions and slow down the rate of corrosion.

List of symbols

K	constant of adsorption equilibrium (dm^3 mol^{-1})
b	Tafel slope (mV)
C	capacity (μF cm^{-2})
CPE	constant phase element
c	concentration (M)
E_a	activation energy (J mol^{-1})
E	potential (mV)
f	frequency (Hz)
j	current density (mA cm^{-2})
L	inductance (H)
R	resistance (Ω)
R	gas constant
iω	complex variable for sinusoidal perturbations with $\omega = 2\pi f$
T	temperature (K)
Z	impedance (Ω cm^2)

Greek letters

Θ	surface coverage (%)
v	scan rate (mV s^{-1})
ω	rotation rate (rad s^{-1})

Sub/superscripts

a	activation
ads	adsorption
b	cathodic
corr	corrosion
i	inhibitor
p	polarization
Ω	ohmic

1. Introduction

Aluminium is a reactive metal with a standard electrode potential of −1.66 V vs NHE. Its resistance against corrosion can be attributed to a rapidly formed thin and highly protective barrier oxide film which separates the bare metal from the corrosive environment. This film can be formed directly in humid air or by exposure to a neutral aqueous electrolyte solution. Protection by this film is very good in environments with pH between 4 and 9, while above and below this range, aluminium exhibits uniform attack [1]. In contrast, a porous and poorly protecting oxide film forms in nonoxidizing acid solutions [2]. However, even in solutions in which the oxide film is stable, the presence of aggressive ions like chloride creates extensive localized attack. It was reported that localized attack occurs by adsorption of chloride ions at weak parts of the oxide film where they act as a reaction partner in the formation of oxide–chloride soluble complexes [3].

The investigations of various aliphatic and aromatic amines, as well as nitrogen-heterocyclic compounds [4–12], showed that their inhibitory action is connected with several factors such as: (i) the structure of the molecules, (ii) the type of adsorption,

(iii) the distribution of charge in the molecule and (iv) the type of interaction between organic molecules and the metallic surface.

In previous work [13, 14] it was shown that substituted *N*-aryl pyrroles acted as cathodic type corrosion inhibitors of aluminium in perchloric acid solution, and of iron corrosion in a strong acid pickling solution. It was found that the position and number of functional groups in pyrrol, or in the benzene ring, strongly influence the inhibition efficiency. In contrast to most commercial acid corrosion inhibitors which are highly toxic, the substituted *N*-aryl pyrroles are nontoxic compounds [15].

The aim of the present work was to study the inhibiting properties of 1-(2-chlorophenyl)–2,5-dimethylpyrrole–3,4-dicarbaldehide (CPMPC) on aluminium covered with a spontaneously formed oxide film in a hydrochloric acid solution. The investigations were performed by means of potentiodynamic and electrochemical impedance spectroscopy (EIS) measurements. In such cases it is important to develop appropriate models for the impedance, which can then be used to fit the experimental data and extract the parameters which characterize the corrosion process [16–19].

2. Experimental details

The aluminium sample selected for the study had the following nominal composition by per cent weight: Al, 99.6; Cu, 0.01; Si, 0.09; Fe, 0.27; Ti, 0.015; V, 0.009. Disc electrodes suitable for the EG&G PARC model 616 system were machined from a cylindrical rod with a diameter of 8 mm. The electrode surface was abraded with emery paper to an 800 metallographic finish, degreased in trichloroethylene and rinsed with triply distilled water. Prior to each electrochemical experiment, the electrode was left for 5 min in the atmosphere and then 2 h in solution. This procedure gave good reproducibility of results. In all measurements the counter electrode was a platinum gauze and the reference electrode was a saturated calomel electrode (SCE). All potential are referred to the SCE.

The measurements were performed in 1 M hydrochloric acid solution without and with the presence of the inhibitor, 1-(2-chlorophenyl)–2,5-dimethylpyrrole–3,4-dicarbaldehide (CPMPC), and in the temperature range 20 to 50 °C. All solutions were deaerated by argon for 30 min before, and during, the measurements. The inhibitor was synthesized by Knorr–Paal condensation with a corresponding amine according to the general method [20, 21]. The product was purified by recrystallization and was identified spectroscopically.

The measurements were carried out in a standard electrochemical cell with a separate compartment for the reference electrode connected with the main compartment via a Luggin capillary. The cell was a water-jacketed version, connected to a constant temperature circulator.

The polarization E against I curves were obtained by means of the linear potential sweep technique with sweep rates of 0.1 mV s^{-1} and 2 mV s^{-1} going from cathodic to anodic side, and with a rotation rate of 2000 min^{-1}. Impedance measurements were performed in the frequency range from 30 mHz to 100 kHz with an a.c. voltage amplitude ± 5 mV. All measurements were performed using a PAR potentiostat, model 273A and a PAR lock-in amplifier, model 5301A with an IBM PS/2 computer.

3. Results and discussion

3.1. *D.c. polarization measurements*

Figure 1 represents the potentiodynamic polarization curves for aluminium in 1 M hydrochloric acid solution with and without the addition of CPMPC in different concentration and at 30 °C. It can be seen that the addition of the inhibitor has almost no influence on the anodic polarization curves. Thus, above −780 mV the polarization behaviour is identical, with or without inhibitor. This means that the inhibitor does not affect the anodic reaction. In contrast, the cathodic current densities decrease as the inhibitor concentration increases.

A similar change in cathodic current density with inhibitor concentration was observed at other temperatures. For example, at 20 °C and at −1.0 V the current density was 27.9 mA cm^{-2} in an uninhibited solution, while in 10^{-6} and 10^{-3} M CPMPC solution, the current density drops to 19.1 mA cm^{-2} and 1.3 mA cm^{-2}, respectively. With increasing temperature the cathodic and anodic current densities also increase, indicating that the corresponding rates of the electrode processes, hydrogen evolution and metal dissolution increase with temperature.

The electrochemical parameters, necessary to consider the kinetics of the corrosion process of the system investigated have been determined from E against log j curves obtained in uninhibited and inhibited hydrochloric acid solutions at all applied

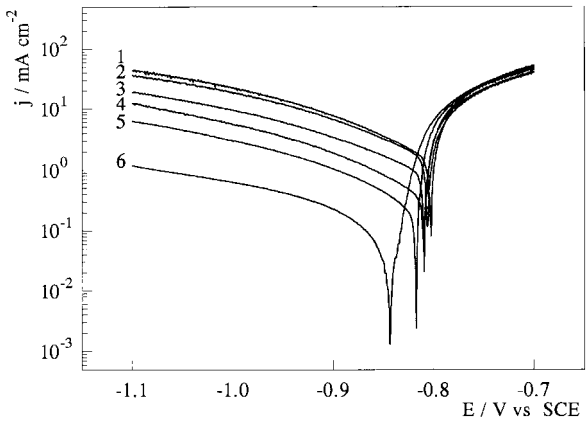

Fig. 1. Tafel plots for aluminium in 1 M hydrochloric acid solution without (1) and in the presence of different concentration of CPMPC (2–6) at t = 30 °C; n = 2000 min^{-1}, v = 2 mV s^{-1}. (2) 1×10^{-6}, (3) 5×10^{-6}, (4) 1×10^{-5}, (5) 1×10^{-4} and (6) 3×10^{-4} M.

temperatures. The dependence of corrosion current and electrode coverage (calculated using the equation $\Theta = 100\,[1 - (j_{corr})_i/(j_{corr})_o]$) on inhibitor concentration are presented in Table 1.

The data on corrosion current densities with and without inhibitor and electrode coverage show that the inhibition efficiency increases with the increase in inhibitor concentration over the whole temperature range.

It is found that data referring to the electrode coverage Θ can be well fitted by the Langmuir adsorption isotherm:

$$c_i\theta = 1/K + c_i \qquad (1)$$

where c_i is the inhibitor concentration and K is the adsorption equilibrium constant.

Figure 2 represents the Langmuir adsorption plot of CPMPC on aluminium in 1 M hydrochloric acid solution at 30 °C. The data obtained give a straight line with the regression coefficient equal to 0.9984. The slope value and the equilibrium constant were determined to be 1.1 and 2.64×10^5 dm^3 mol^{-1}, respectively. Electrode coverage at the other temperatures obeyed the Langmuir adsorption plot too. The results obtained indicate that the inhibitory action of CPMPC occurs by simple blocking of the electrode surface.

As can be seen from Fig. 1, the cathodic Tafel slope is almost equal in uninhibited and inhibited solutions. It increases somewhat with temperature and by increasing temperature the scattering is larger. The large Tafel slopes b_c (between 180 and 300 mV div^{-1}) indicate that the hydrogen evolution reaction occurs at the metal covered by a surface layer, probably an oxide inhibitor complex, which acts as a potential energy barrier to the charge carriers [22, 23].

Since the polarization measurements were performed in deaerated solution and with a rotating disc electrode ($n = 2000$ min^{-1}), the only cathodic process occurring at the metal–solution interface was a hydrogen evolution reaction. The fact that b_c values are almost the same in uninhibited and inhibited solutions suggests that the inhibitory action of CPMPC improves dielectric properties (barrier characteristics) of the surface layer without affecting the reduction mechanism.

The barrier-film model is a consistent way of explaining the observed high Tafel slopes for the hydrogen evolution reaction. It assumes that a fraction of the applied electrode overpotential operates across the surface film and hence is not available to assist the charge transfer (hydrogen evolution reaction) at the film solution interface [22, 23].

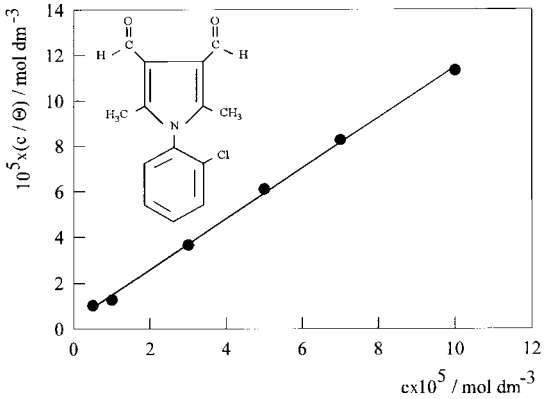

Fig. 2. Langmuir plot for the adsorption of CPMPC on aluminium from 1 M hydrochloric acid solution at 30 °C. $K = 1.55 \times 10^5$ mol^{-1} dm^3.

In the present work the energy of activation of the hydrogen evolution reaction was calculated from the slope of log j_c against $1/T$ straight line, according to the equation:

$$\log j_c = E_a/(2.3RT) + \text{constant} \qquad (2)$$

where j_c is the cathodic current and E_a is the activation energy.

The activation energy at constant inhibitor activity on the metal surface, that is, at a constant degree of surface coverage were determined in order to eliminate the influence of temperature on the protection efficiency and degree of surface coverage [24]. From the Arrhenius plot the activation energy values at various surface coverage were calculated. The value obtained (50 ± 5 kJ mol^{-1}) shows that there is no difference between activation energies of uninhibited and inhibited reaction suggesting again that the inhibition does not affect the reaction mechanism of the hydrogen evolution reaction.

3.2. *Electrochemical impedance spectroscopy measurement*

The impedance spectra obtained on aluminium in 1 M hydrochloric acid solution at different potentials are presented in a three-dimensional diagram in Fig. 3. Characteristic values of Z_f and polarization resistance (R_p) are defined by the equation [25]:

$$R_p = \lim_{\omega \to 0} \mathrm{Re}\,\{Z_f\} \qquad (3)$$

where $\mathrm{Re}\{Z_f\}$ denotes the real part of the complex faradaic impedance Z_f and ω corresponds to the frequency of the a.c. signal ($\omega = 2\pi f$).

At cathodic polarization ($E = E_{corr} - 80$ mV) a Nyquist plot, (Fig. 3(a)), exhibits only semicircular

Table 1. Corrosion currents and inhibition efficiencies for aluminium in 1 M hydrochloric acid without and with the presence of various concentration of CPMPC at 30 °C

c (*CPMPC*)/mol dm^{-3}	0	1×10^{-6}	1×10^{-5}	3×10^{-5}	5×10^{-5}	7×10^{-5}	1×10^{-4}
j_{corr}/mA cm^{-2}	2.028	1.044	0.435	0.371	0.369	0.311	0.238
Θ/%	–	48.52	78.55	81.70	81.80	84.68	88.26

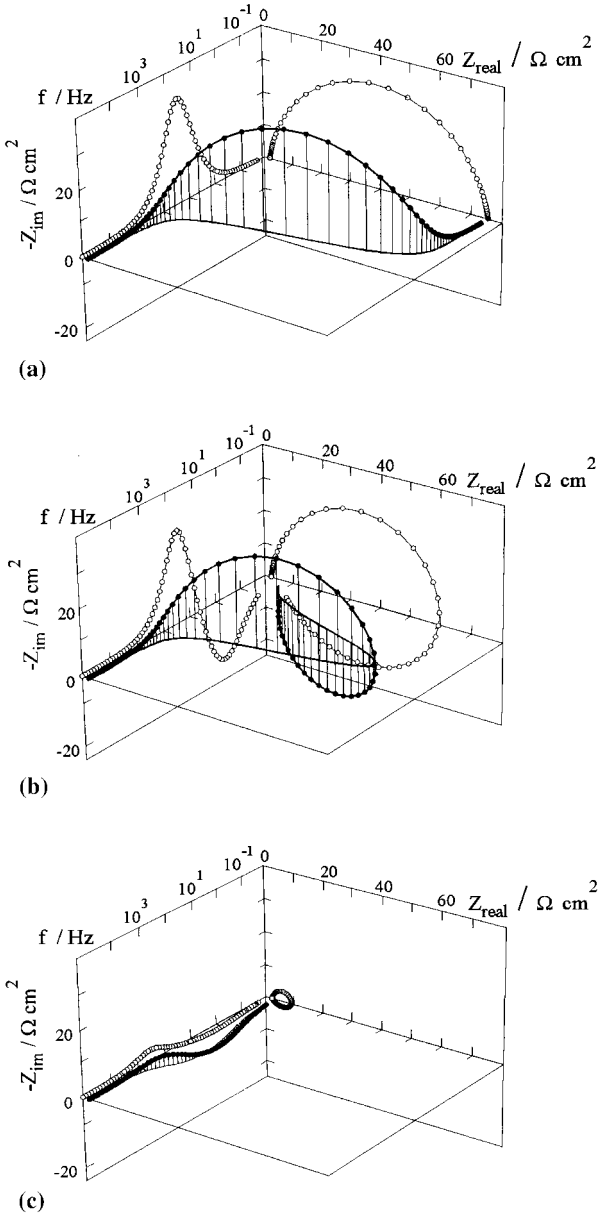

Fig. 3. Tridimensional impedance plot for aluminium in 1 M hydrochloric acid solution at 20 °C, and at: (a) −80 mV from the E_{corr}, (b) at E_{corr}, and (c) at +60 mV from the E_{corr}.

behaviour, indicating that the hydrogen evolution reaction on the electrode surface under the cathodic polarization is under the charge transfer control.

At the corrosion potential (E_{corr}) a Nyquist plot shows a large semicircular capacitive loop at high frequency which is then followed by a large inductive loop (Fig. 3(b)). For $\omega \to 0$, the impedance intersects the real axis at a point which is close to the solution resistance (R_Ω). This represents the polarization resistance (R_p) of the corrosion process, which is defined by Equation 3.

At a low anodic polarization ($E = E_{corr} + 60$ mV) the rate of the faradaic process of localized corrosion increases in the presence of Cl^- ions and the corresponding capacitive loop is strongly reduced (Fig. 3(c)). In this case, at $\omega \to 0$ the impedance intersects the real axis at a point which almost matches the solution resistance giving R_p which is almost equal to R_Ω.

At the first sight two time constants can be observed in Fig. 3(b): (i) a time constant at high frequencies corresponding to the capacitive loop and (ii) a time constant at low frequency corresponding to the inductive loop. At present time the origin of the different time constants is not clear. According to Bessone *et al.* [26] and Wit *et al.* [27], the high frequency time constant could be attributed to the oxide layer on aluminium. Brett [28], however, has reported that this time constant could be assigned to the interfacial reactions, in particular the metal oxidation reaction at the metal–oxide interface. He suggested that aluminium is oxidized to Al^+ intermediates which are subsequently oxidized to Al^{3+} ions. As far as the inductive loop is concerned, Burnstein's measurements [29, 30] have indicated that the loop is closely related to the existence of a passive film on aluminium. Lenderink *et al.* [31] have attributed this loop to the relaxation of adsorbed species like H^+_{ads}. Inductive behaviour is also observed for the pitted active state and attributed to the surface area modulation or salt film property modulation [32]. Keddam *et al.* [33] have given the same hypothesis for the anodic dissolution of aluminium in acidic sodium chloride solution.

The influence of CPMPC on impedance spectra of aluminium in 1 M HCl solution at the E_{corr} is shown in Fig. 4 in a Nyquist (a) and Bode (b) plots, respectively. In the Bode plot the high frequency limit corresponds to the electrolyte resistance R_Ω. The low frequency limit represents the sum of R_Ω and R_p, which is generally determined by both the electronic or ionic conductivity of the surface film and the polarization resistance. The phase angle against log f plot shows the phase angle dropping zero at high and low frequencies, corresponding to the resistive behaviour of R_Ω and (R_Ω + R_p). By increasing inhibitor concentration the polarization resistance, R_p increases. The medium frequency range is determined by the capacitance C and the phase angle rises towards −90°.

The increase of both the capacitive loop and the polarization resistance can be observed in the Nyquist plot. As in the previous case, the inductive part of the impedance was mainly determined by the relaxation process of hydrogen and Cl^- adsorption, and Al-dissolution, while the high frequency time constant can be correlated with the dielectric properties of a surface layer; i.e. [metal–oxide–hydroxide–inhibitor]$_{ads}$ complex.

Influence of a longer immersion time on the impedance spectra of aluminium in inhibited hydrochloric acid solution is shown in Fig. 5. The impedance spectra show that the protective properties of a phase layer increase, the layer resistance and the exponent of the constant phase element increase, while its capacitance decreases.

Figures 3, 4 and 5 show clearly that the semicircles obtained are depressed. Deviations of this kind, often

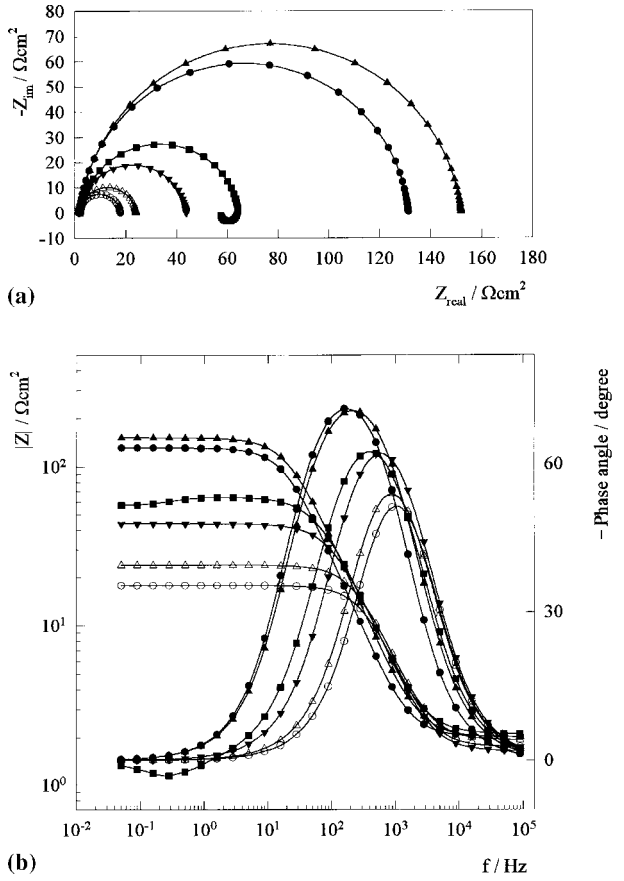

Fig. 4. Nyquist plots (a) and Bode plots (b) for aluminium in 1 M hydrochloric acid solution at E_{corr} without (○) and in the presence of: (△) 1×10^{-5}, (▼) 5×10^{-5}, (■) 1×10^{-4}, (●) 3×10^{-4} and (▲) 5×10^{-4} M CPMPC at 30 °C.

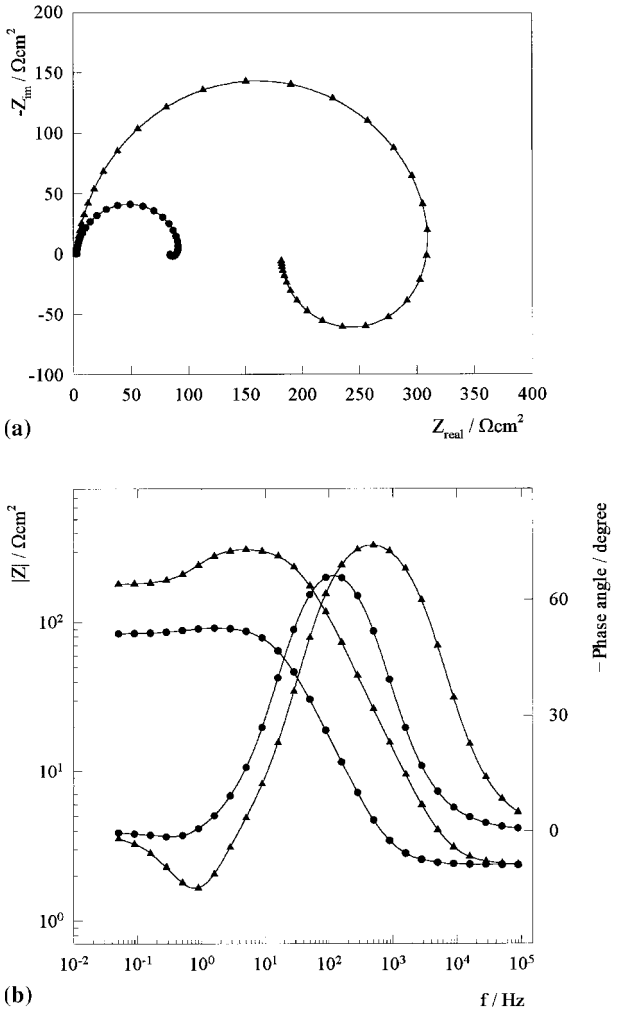

Fig. 5. Nyquist plot (a) and Bode plot (b) for aluminium in 1 M hydrochloric acid solution obtained after 2 (●) and 70 h (▲) immersion at E_{corr} in the presence of 5×10^{-4} M CPMPC at 30 °C.

referred to as frequency dispersion, have been attributed to inhomogeneities of the solid surfaces as the aluminium surface is always [34]. A practical way to represent distributed processes such as corrosion of a rough and inhomogeneous electrode is with an element that follows its distribution. The constant phase element (CPE) meets that requirement. The impedance of CPE takes the form:

$$Z_{CPE} = (A(i\omega)^n)^{-1} \quad (4)$$

where the coefficient A is a combination of properties related to both the surface and the electroactive species. The exponent n has values between −1 and 1. A value of −1 is characteristic of an inductance, a value of 1 corresponds to a capacitor, a value of 0 corresponds to a resistor and a value of 0.5 can be assigned to diffusion phenomena. For $n = 1$ and $n = -1$, the above equation becomes: $Z_C = (Ci\omega)^{-1}$ and $Z_L = Li\omega$, respectively, where L is the inductance.

Figure 6 represents the equivalent circuit used to fit the experimental data. This consists of CPE_1 in parallel to the series resistors R_1 and R_2, and a CPE_2 in parallel to R_2.

For each set of experimental data in Figs 3–5, the parameters R_1, R_2, CPE_1 and CPE_2 were evaluated using a simple least square fit procedure and are listed in Tables 2–4. The experimental data were found to be sufficiently well fitted by the transfer function of

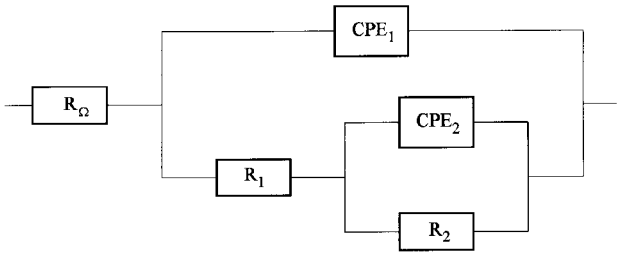

Fig. 6. Equivalent circuit diagram.

Table 2. Impedance parameters for aluminium in 1 M hydrochloric acid solution at different potentials and at 20 °C

Impedance parameters	*Potential vs E_{corr}*/V		
	−80 mV	*E_{corr}*	*+60 mV*
R_Ω/Ω cm^2	2.0	2.2	2.2
10^{-6} CPE_1/Ω^{-1} cm^{-2} s^n	155	154	157
n_1	0.898	0.924	0.888
R_1/Ω cm^2	73.5	2.16	0
R_2/Ω cm^2	–	60.92	7.69
CPE_2/Ω^{-1} cm^{-2} s^n	–	3.64×10^{-2}	3.84×10^{-1}
n_2	–	−0.709	−0.545

Table 3. Impedance parameters for aluminium in 1 M hydrochloric acid solution without and with the presence of various concentrations of CPMPC at E_{corr} and at 30 °C

c/mol dm^{-3}	R_Ω/Ω cm^2	10^{-6} CPE_1 /Ω^{-1} cm^{-2} s^n	n_1	R_1/Ω cm^2	R_2/Ω cm^2	CPE_2 /Ω^{-1} cm^{-2} s^n	n_2
0	1.7	48.0	0.947	16.1	–	–	–
5×10^{-6}	1.9	48.1	0.940	15.9	–	–	–
1×10^{-5}	1.9	48.3	0.941	22.0	–	–	–
3×10^{-5}	1.8	62.6	0.892	50.9	–	–	–
5×10^{-5}	1.6	60.5	0.927	42.1	–	–	–
7×10^{-5}	2.4	64.9	0.906	62.4	1.4	1.400	−1.000
1×10^{-4}	2.1	67.2	0.919	61.1	7.4	0.270	−0.995

Table 4. Impedance parameters for aluminium after 2 and 70 h of immersion in 1 M hydrochloric acid solution with 5×10^{-4} M CPMPC at E_{corr} and at 30 °C

t/h	R_Ω/Ω cm^2	10^{-4} CPE_1 /Ω^{-1} cm^{-2} s^n	n_1	R_1/Ω cm^2	R_2/Ω cm^2	CPE_2 /Ω^{-1} cm^{-2} s^n	n_2
0	2.4	1.46	0.933	81.4	10	0.370	−0.969
70	2.4	0.21	0.933	178.7	139	0.052	−0.991

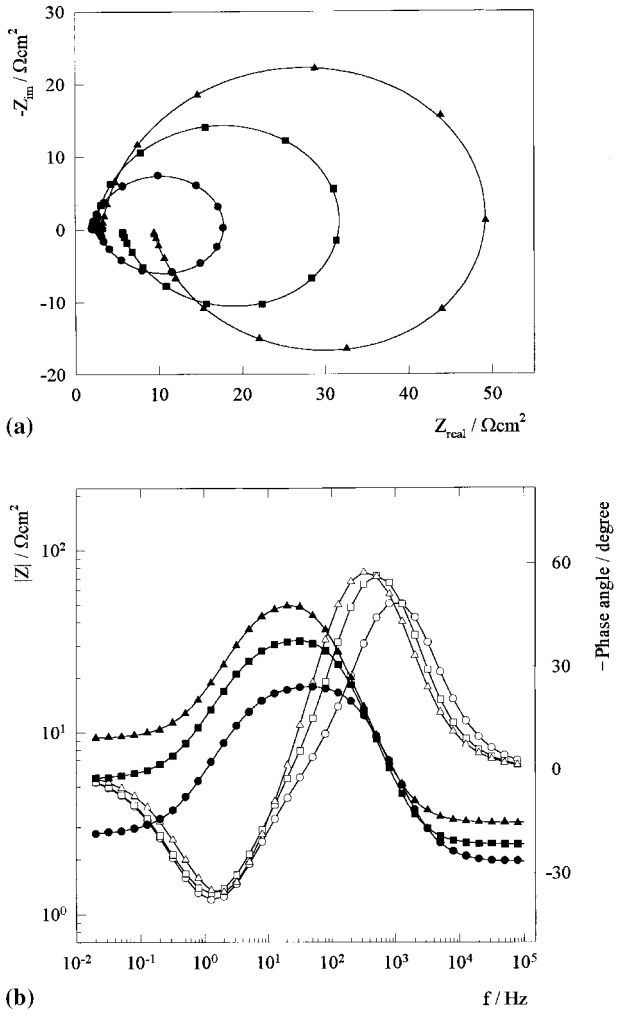

Fig. 7. Nyquist plots (a) and Bode plots (b) for aluminium in 1 M hydrochloric acid solution at E_{corr} + 15 mV without (●) and in the presence of (■) 10^{-6} and (▲) 10^{-5} M CPMPC at 30 °C

the equivalent circuit presented in Fig. 6 within the limits of experimental error and reproducibility of data.

The effect of increasing the CPMPC concentration on the impedance spectra obtained at small anodic polarization ($E = E_{corr} + 15$ mV) at 30 °C are presented in Fig. 7. The impedance spectra were analysed according to the equivalent circuit in Fig. 6 and the circuit parameters are presented in Table 5.

With an increase in inhibitor concentration the capacitive loop increases more strongly than the corresponding R_p value, indicating that the adsorbed molecules of CPMPC on the electrode surface have almost no influence on the rate of the anodic process.

4. Conclusions

The inhibiting action and the adsorption behaviour of CPMPC on aluminium was investigated in a hydrochloric acid solution by means of potentiodynamic and impedance measurements.

Polarization measurements show that the addition of inhibitor induces a decrease in the cathodic cur-

Table 5. Impedance parameters for aluminium in 1 M hydrochloric acid solution with and without the presence of CPMPC at E_{corr} + 15 mV and at 30 °C

Impedance parameters	*Concentration of inhibitor*/mol dm^{-3}		
	nil	1×10^{-6}	1×10^{-5}
R_Ω/Ω cm^2	2.0	2.1	2.4
10^{-6} CPE_1/Ω^{-1} cm^{-2} s^n	59.5	86.2	56.6
n_1	0.921	0.942	0.951
R_1/Ω cm^2	0.8	2.4	3.1
R_2/Ω cm^2	16.0	32.2	28.3
CPE_2/Ω^{-1} cm^{-2} s^n	0.99	0.34	0.51
n_2	−0.830	−0.866	−0.829

rents without affecting the anodic polarization behaviour. The adsorption behaviour of CPMPC follows a Langmuir adsorption isotherm with an equilibrium constant $K = 1.1–2.64 \times 10^5\ dm^3\ mol^{-1}$.

Impedance measurements performed at E_{corr} and at small anodic polarization show a high frequency capacitive behaviour related to the dielectric properties of the surface film and a low frequency inductive part related to the relaxation of adsorbed species. Electrical parameters of the proposed equivalent circuit are calculated and presented.

The results show that the inhibitory action increases with increasing concentration of CPMPC and immersion time and decreases with increasing temperature.

Acknowledgement

This work was supported by the Ministry of Science of the Republic of Croatia through grant 125011.

References

[1] M. Pourbaix, 'Atlas of Electrochemical Equilibrium Diagrams in Aqueous Solutions', NACE, Houston, Texas (1966), p. 499.
[2] R. S. Alwitt, in 'Oxides and Oxide Films', Vol.6 (edited by J.W.Diggle and A.K.Vijh), Marcel Dekker, New York (1976), p. 169.
[3] F. D. Bogar and R. T. Foley, *J. Electrochem. Soc.* **119** (1972) 462.
[4] G. Trabanelli, in 'Corrosion Mechanisms' (edited by F. Mansfeld), Marcel Dekker, New York (1987), p. 119.
[5] S. L. Granese, *Corros. Sci.* **44** (1988) 322.
[6] S. L. Granese and B. M. Rosales, Proceedings of the 7th European Symposium on 'Corrosion Inhibitors', Ann. Univ. Ferrara, N.S., Sez. V, Suppl. N.9 (1990), p. 73.
[7] M. N. Desai, B. C. Thakar, P. M. Chhaya and M. H. Gandhi, *Corros. Sci.* **16** (1976) 9.
[8] C. Monticelli, G. Brunoro and G. Trabanelli, Proceedings op. cit. ref. [6], p. 1125.
[9] T. M. Salem, J. Horvath and P. S. Sidky, *Corros. Sci.* **18** (1978) 363.
[10] D. Tromans, *Corrosion* **42** (1986) 601.
[11] F. Tirbonod and C. Fiaud, *Corros. Sci.* **18** (1978) 139.
[12] L. Garrigues, N. Pebere and F. Dabosi, *Electrochim. Acta* **41** (1996) 1209.
[13] Z. Grubač, M. Metikoš-Huković, E. Stupnišek-Lisac and J. Vorkapić, Proceedings of Eurocorr 1991, Budapest (1991), p. 105.
[14] E. Stupnišek-Lisac, M. Metikoš-Huković, D. Lenčić and J. Vorkapić-Furač, *Corrosion* **48** (1992) 924.
[15] J. A. Maga, *J. Agric. Food Chem.* **29** (1981) 691.
[16] J. R. Macdonald, 'Impedance Spectroscopy', J. Wiley & Sons, New York (1987).
[17] K. Juttner, *Electrochim. Acta* **35** (1990) 1501.
[18] W. J. Lorentz and F. Mansfeld, *Electrochim. Acta* **31** (1986) 467.
[19] F. Mansfeld, *ibid.* **35** (1990) 1533.
[20] J. Vorkapić-Furač, M. Mintas, T. Burgenmeister and A. Mannschreck, *J. Chem. Soc. Perkin Trans.* **2** (1989) 713.
[21] K. Imuro and T. Hanafusa, *Bull. Chem. Soc. Jpn* **49** (1976) 1364.
[22] A. K. Vijh, *J. Phys. Chem.* **73** (1969) 506.
[23] R. E. Mayer, *J. Electrochem.* Soc. **113** (1966) 1158.
[24] B. G. Ateya, B. E. Anadouli and F. M. Nizamy, *Corros. Sci.* **24** (1984) 497, 509.
[25] W. J. Lorentz and F. Mansfeld, *ibid.* **21** (1981) 647.
[26] J. Bessone, C. Mayer, K. Juttner and W. J. Lorenz, *Electrochim. Acta* **28** (1983) 171.
[27] H. J. Witt, C. Wijenberg and C. Crevecoeur, *J. Electrochem. Soc.* **126** (1979) 779.
[28] C. M. Brett, *Corros. Sci.* **33** (1992) 203; *idem*, *J. Appl. Electrochem.* **20** (1990) 1000.
[29] G. T. Burnstein and R. J. Cinderey, *Corros. Sci.* **33** (1992) 475.
[30] G. T. Burnstein and R. J. Cinderey, *ibid.* **32** (1991) 1195.
[31] H. J. W. Lenderink. M. V. D. Linden and J. H. Witt, *ibid.* **38** (1993) 1989.
[32] J. B. Bessone, D. R. Salinas, C. Mayer, M. Ebert and W. J. Lorenz, *Electrochim. Acta* **37** (1992) 2283.
[33] A. Frichet, P. Gimenez and M. Keddam, *ibid.* **38** (1993) 1957.
[34] A. Despić and V. P. Parkhutik, in 'Modern Aspects of Electrochemistry', Vol. 20 (edited by J. O'M. Bockris, R. E. White and B. E. Conway), Plenum Press, New York (1989), p. 401.